Contents lists available at ScienceDirect

Separation and Purification Technology

Transforming wastewater ammonia to carbon free energy: Integrating fuel cell technology with ammonia stripping for direct power production

C.J. Davey , B. Luqmani , N. Thomas , E.J. McAdam [*]

Cranfield Water Science Institute, Cranfield University, Bedfordshire MK43 0AL, UK

ABSTRACT

The transformation of ammonia from pollutant to energy rich carbon free fuel presents an opportunity for the transition of wastewater services to net zero. However, there is only limited knowledge of how the product quality of ammonia recovered from real wastewater might impact on its downstream exploitation in fuel cells. This study therefore exploited vacuum stripping to produce an aqueous ammonia concentrate from real wastewater that was then evaluated within a direct ammonia fuel cell, as a reference technology for energy generation. A 17 g L^{-1} aqueous ammonia product was created by vacuum stripping centrate from a full-scale anaerobic digester (2 gN L^{-1}). The pH of the product was lower than expected due to the mild-acidification of solution by the co-transport of low MW volatile organic compounds. This reduced power density in the fuel cell, due to the incomplete deprotonation of ammonia (lowering oxidation potential at the fuel cell anode) and a decrease in [OH$^-$] which is required for complete electrochemical conversion. We propose that improved vacuum stripping design can increase the distillate ammonia concentration and produce a more alkaline product, yielding markedly higher fuel cell power density by enhancing ammonia oxidation at the anode (through concentration and deprotonation) and reducing [OH$^-$] mass transfer limitations. As the separation energy for ammonia is dominated by the latent heat demand of water vapour, a synergy exists between creation of a concentrated ammonia product (that improves power density) and reducing the energy demand for separation. The energy balance from this research evidences that despite the high latent heat demand for separation, the low cost of heat coupled with the power produced from ammonia yield a favourable economic return when compared to conventional biological treatment. This study also identifies that revaluing ammonia as a carbon free fuel can help reposition wastewater treatment for a zero-carbon future.

1. Introduction

Ammonia oxidation is energy intensive, constituting around one-third of the aeration required in activated sludge, which collectively demands 60% of the total energy requirement for wastewater treatment [1]. Stricter wastewater regulations have been imposed in the EU reducing ammonia nitrogen discharge limits from 25 to 8 mg L^{-1} [2]. Consequently, the drive towards tighter compliance standards necessitates a considerable increase in energy demand, at a time where the water sector has stated ambitions for delivering energy neutrality and net zero [3]. In the energy sector, ammonia is viewed as a next generation carbon free fuel, which offers a higher volumetric energy density than hydrogen [4]. With over ten billion litres of wastewater produced in England and Wales each day, the potential energy associated with ammonia equates to ~1 TW h y^{-1} [5]. This exceeds energy production from renewables currently operated by the water industry (0.49 TW h

y^{-1}), as is equivalent to over 40% of sector wide energy consumption (2.3 TW h y^{-1}) [5]. Therefore, while ammonia can be recovered for use as a fertiliser or generic industrial feedstock [6], by revaluing ammonia as carbon free fuel, the water industry has access to an entirely new renewable energy resource. Ammonia recovery also eliminates the energy demand for the biological oxidation of ammonia, and thus the associated nitrous oxide emissions (a potent greenhouse gas). Consequently, 'ammonia-to-energy' can create a triple carbon benefit for the transition to net zero.

While fuel cell technology has seen widespread development for exploitation in the ammonia economy, the application of this technology for direct power generation using wastewater derived ammonia is an emerging field. Zhang et al. (2020) studied a direct ammonia fuel cell (DAFC) for power generation from landfill leachate to provide electrical energy generation coupled with ammonia oxidation [7]. Although leachate has an ammonia concentration which is considerably higher
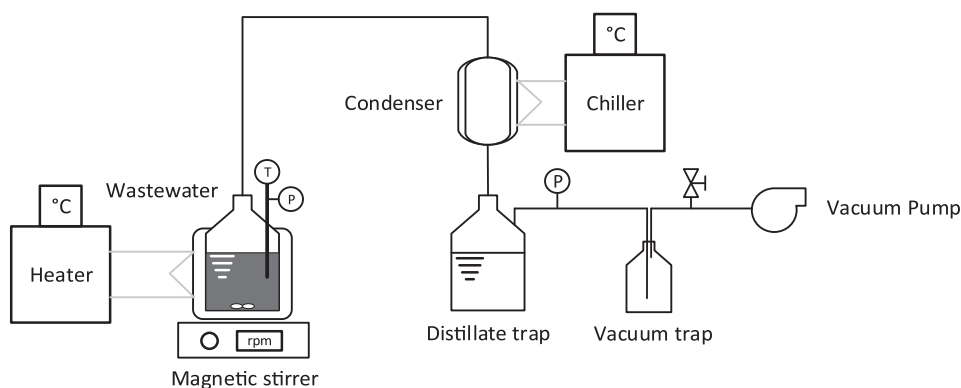
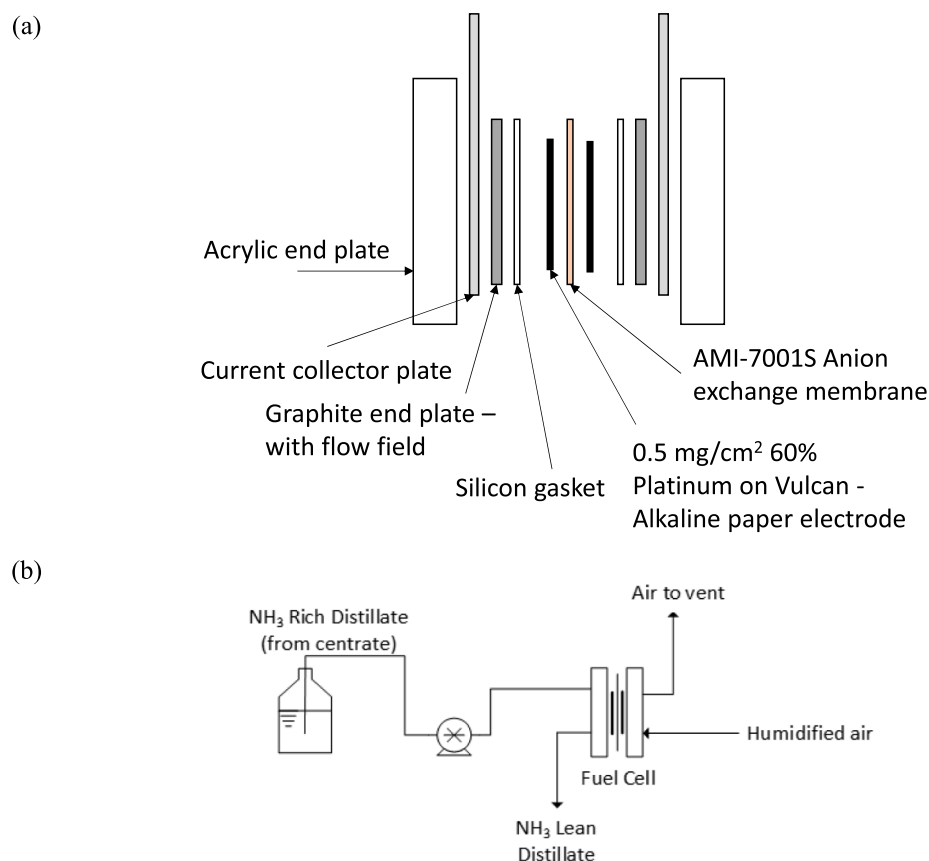**Fig. 1.** Schematic of the vacuum thermal stripping experimental set-up.

Fig. 2. Schematic of the direct ammonia fuel cell experimental set-up: (a) breakdown of the direct ammonia fuel cell and (b) diagram of the experimental set-up.

than municipal wastewater (~2 g L^{-1}; 0.12 M), fuel cell power density was shown to significantly improve with further increase in ammonia concentration. Distinction in power density between real leachate and synthetic leachate of similar concentration also implied that the background matrix interfered with oxidation, which may be due to fouling, material degradation or redox competition from the more complex liquid matrix. By analogy, for direct urea fuel cells, the separation and purification of urea from urine has been proposed to avoid electrode contamination from the organic and inorganic constituents in urine which reduce urea oxidation kinetics [8]. The separation, concentration and purification of ammonia prior to fuel cell application will therefore advantage energy recovery. Ammonia stripping is presently the most advanced concentrative technology to facilitate transformation of ammonia into a product for use in fuel cells. However, the low

dimensionless Henry's law constant for ammonia evidences that mass transfer is strongly dependent on concentration. Consequently, this favours application to centrate from return liquors, where up to one-third of the ammonia load is present in <1% of the flow, or to waste streams arising from ion exchange or electrodialysis (ED) processes which can preconcentrate ammonia from the main wastewater flow, but to only a limited concentration threshold (~7 g L^{-1}) [9–11].

While two-stage ammonia stripping/acid scrubbing is often applied to concentrated liquors, the dilute acidic aqueous phase that is produced is not conducive to fuel cell application [12]. Steam stripping can produce a more concentrated aqueous phase, but the steam load required for high separation efficiency (70–140 kg m^{-3}) limits application to all but the most concentrated industrial feeds [13]. Thermal vacuum stripping lowers the boiling point of solution to ~60 °C, which permits

Table 1
Details of the anion exchange membrane used.

Membrane characteristics	Detail
Manufacturer	Membranes International Inc.
Name	AMI-7001
Functionality	Strong Base Anion Exchange Membrane
Polymer Structure	Gel polystyrene cross linked with divinylbenzene
Functional Group	Quarternary Ammonium
Standard Thickness (mm)	0.45 ± 0.025
Electrical Resistance (Ohm cm^2) 0.5 mol/L NaCl	<40
Maximum Current Density (A m^{-2})	<500
Permselectivity (%) 0.1 mol KCL/kg/0.5 mol KCl/kg	90
Total Exchange Capacity (meq/g)	1.3 ± 0.1
Water permeability (ml/hr/ft^2) @5psi	>80
Thermal Stability (°C)	90

use of waste heat from biogas facilities co-located with return liquors, enabling a large reduction in separation energy requirement, where production of a concentrated aqueous ammonia product up to 6.4 M (109 g L^{-1}) has been demonstrated [14]. Unlike other ammonia recovery methods, thermal stripping technology is less sensitive to influent solids, while the lower stripping temperatures and avoidance of air in vacuum stripping can also avoid the problems of scaling [15]. The capacity for this technology to facilitate highly selective ammonia separation (concentration factor > 50) is important as it may improve fuel cell efficiency, reduction in the co-transport of water will also lower the latent heat demand for separation, but the thermal driving force could encourage the co-transport of unwanted low molecular weight organics.

Stoeckl et al. [16] proposed using vacuum membrane distillation for the recovery of ammonia from wastewater as a purified and concentrated humidified gas so that the ammonia/water gas mixture could be applied directly to a solid oxide fuel cell (SOFC) for energy generation. The authors demonstrated fuel cell degradation over 1000 h from the synthetic ammonia/water mixture that was similar to degradation observed with a hydrogen/nitrogen mixture [16]. Van Linden et al. [17] coupled vacuum membrane stripping and SOFC for ammonia recovery from synthetic feeds with varying ammonia concentrations. Due to the

high operating temperature requirements for SOFC (>500 °C), DAFCs are also under development for gaseous and aqueous ammonia fuel [12] which offer a potential advantage due to comparatively faster start-up [18]. DAFC employ alkaline exchange membranes (AEM) at moderate temperatures to mediate ammonia oxidation at the anode and reduction of oxygen at the cathode [19], which can deliver economically practicable power densities [18]. As most materials such as metals, alloys, oxides and hydroxides are chemically stable in an alkaline environment, DAFC with AEM allows for a wide choice of electrocatalysts [20]. The fuel cell efficiency could be reduced by ammonia permeability of the AEM and thus the composition of the fuel mixture and choice of electrocatalysts can influence the electrochemical performance of DAFC [21]. To date, fuel cell degradation by the fuel mixture has driven research to identify suitable electrocatalysts for the cathode [22–24], anode [25,26] and electrolyte [27]. However, these studies are generally limited to examination of the impact on fuel cell stability by the primary fuel mixture (i.e., ammonia), which is controlled by blending pure gases to create a synthetic feed. The use of synthetic feeds cannot infer the consequence of developing ammonia rich fuels from wastewater, where pre-concentration *via* thermal separation can promote the co-transport of volatile organic compounds (e.g., alkanes, alkenes, and aromatics) and dissolved gases [28] which may influence the fuel chemistry and fuel cell functionality.

While the concept of wastewater ammonia for energy generation has been previously described [16,17], to the authors knowledge, the thermal recovery of a purified ammonia product from real wastewater combined with its direct utilisation for electrical energy generation in a fuel cell has yet to be described. The aim of this study is therefore to establish how thermal separation of ammonia from wastewater may influence the product characteristics for power generation, by using a DAFC as a reference system to examine fuel cell efficiency. To achieve this aim, thermal vacuum stripping is used to produce an ammonia concentrate using return liquor (centrate) generated from a full-scale anaerobic digestion facility. The objectives are to: (i) recover a concentrated and purified aqueous ammonia product from real wastewater using thermal vacuum stripping; (ii) characterise the impact of aqueous ammonia feed chemistry on power and energy generation using DAFC as a reference fuel cell; (iii) evidence the presence and potential impact of co-transported compounds on reference fuel cell performance;
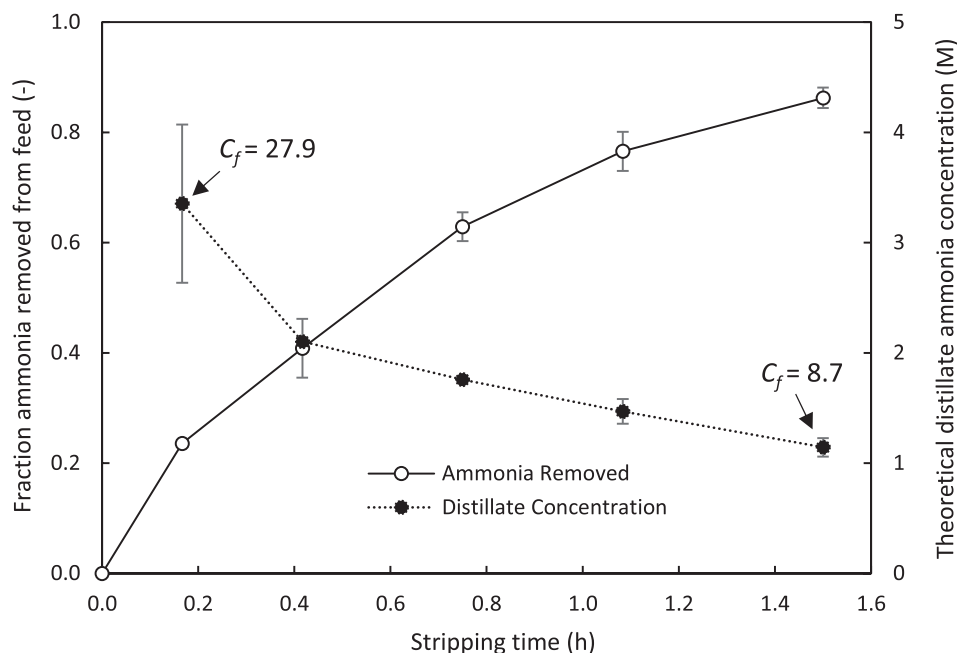

Fig. 3. Ammonia concentration in wastewater and distillate over time during the batch vacuum thermal stripping showing the initial concentration factor (Cf) of the distillate being 27.9 and the final 9.5 (stripping temperature = 65 °C, Pressure = 0.25 bar$_a$.

Table 2
Solution characteristics of the wastewater, recovered distillate and synthetic ammonia solutions.

Parameter	Solution			
	Wastewater centrate	*Wastewater ammonia distillate*	*1 M NH₃*	*1 M NH₃ + 1 M KOH*
NH_3 (g L^{-1})	2.010 ± 0.010	17.3	17.03	17.03
pH	8.0 ± 0.01	10.5	11.83	14.43
Conductivity (mS cm^{-1})	14.6 ± 0.1	26.2 ± 0.14	1.2 ± 0.0078	186 ± 0.22
UV$_{254nm}$ (%T)	5.83*	29.6	100	100
Total COD (mg L^{-1})	5773 ± 598	248 ± 1.0	–	–
Soluble COD (mg L^{-1})	2791 ± 534	243 ± 5.0	–	–
Total Solids (mg L^{-1})	4900 ± 265	–	–	–
Total Suspended Solids (mg L^{-1})	273 ± 64	–	–	–
Total inorganic carbon (as C) (mg L^{-1})	1659 ± 7	–	–	–
Alkalinity (as CaCO₃) (mg L^{-1})	6875 ± 569	–	–	–
Solution Surface Tension (mN m^{-1})	44.5	51	69	–

*Measured at 1/10 dilution and factorised; – not measured).
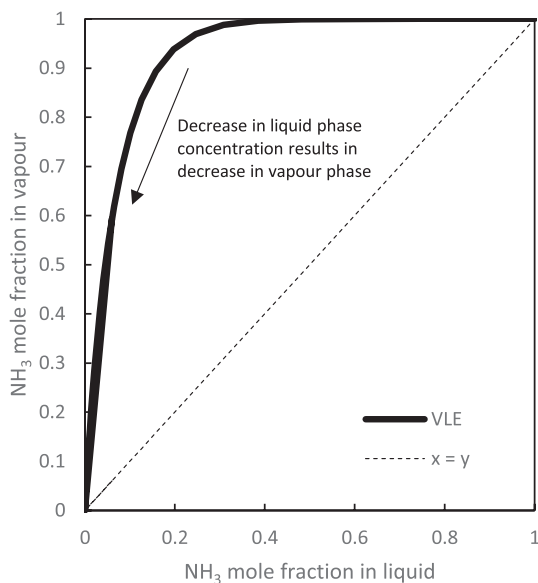

Fig. 4. Vapor-liquid equilibrium of ammonia-water demonstrating the change in vapor phase concentration as the liquid phase concentration decreases during the batch thermal stripping process. Calculated using the function presented in [30].

and (iv) discuss the potential for integrating fuel cell technology to thermal stripping to describe the energy and carbon benefits, but also the critical interactions which may serve to improve associated sustainability criteria to allow the water industry to take advantage of this carbon free fuel for the transition to net-zero.
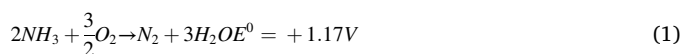
2. Materials and methods
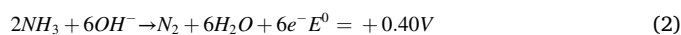
2.1. Experimental set-up

The vacuum distillation set-up comprised a 1 L jacketed vessel,

operated at 0.5 L capacity, and agitated using a magnetic stirrer plate at ~450 rpm (SB151, Stuart, Stone, UK) (Fig. 1). The feed was initially heated to 65 ± 0.5 °C (MPC-K6, Huber, Offenburg, Germany) under atmospheric conditions, and slowly reduced to 250 ± 5 mbar using a vacuum pump (ME-1C, Vacuubrand, Wertheim, Germany). Temperature and pressure were continuously monitored (Type K, RS Components, Corby, UK; PXM319-010GI, Omega Engineering Ltd, Manchester, UK). The pH was fixed to pH11. Ammonia-rich vapour was condensed (Scilabware Ltd., Stoke-on-Trent, UK) at 5 °C. The ammonia-rich condensate was collected and stored in a jacketed vessel at 5 °C to prevent volatilisation.
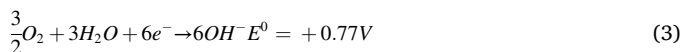
The direct ammonia fuel single cell (Fig. 2a) was adapted from a commercially available electrochemical cell kit (Flex-Stak Electrochemical Cell, Fuel Cell Store, USA) consisting of two acrylic end plates, two current collectors, two graphite end plates with a flow field and a single membrane electrode assembly (MEA). The active surface area of the MEA was 10 cm². Alkaline electrodes were applied with 60% PtC coated at 0.5 mg cm^{-2} on carbon paper (Fuel Cell Store, US). The gas diffusion layer of these electrodes consisted of PTFE treated carbon paper that is 200 μm thick. Although more efficient electrocatalysts for ammonia oxidation have been demonstrated, Pt was chosen due to its commercial availability and previous benchmarking in DAFCs [27]. An AMI-7001 (Membranes International Inc., USA) anion exchange membrane was soaked in 1 M KOH for 24 h before use (Table 1). The overall reaction for the fuel cell is:

$$2NH_3 + \frac{3}{2}O_2 \rightarrow N_2 + 3H_2O \quad E^0 = +1.17V \tag{1}$$

with the anodic reaction as:

$$2NH_3 + 6OH^- \rightarrow N_2 + 6H_2O + 6e^- \quad E^0 = +0.40V \tag{2}$$

and cathodic reaction as:

$$\frac{3}{2}O_2 + 3H_2O + 6e^- \rightarrow 6OH^- \quad E^0 = +0.77V \tag{3}$$

Solutions were preheated to 40 °C (StableTemp, Cole Parmer, UK) and passed through the fuel cell at 5 mL min^{-1} using a peristaltic pump (520Du, Watson Marlow, UK). Prehumidified air supplied oxygen to the cathode at a flow rate of 3 L min^{-1} set by rotameter (0.4–5 L min^{-1}, Cole Parmer, UK). This ensured an excess stoichiometric flow of oxygen to ammonia. The fuel cell was left to equilibrate for at least 10 min, with equilibrium confirmed by a stable open circuit voltage (OCV). Polarisation curves were conducted using current steps between 0.1 and 0.5 mA with each step sustained for 60 s to stabilise the potential. All electrochemical measurements were conducted using a galvanostat (Iviumstat.h, Alvatek, UK). Following fuel cell assembly, the cell was benchmarked with a solution comprising 5 M NH₃ and 1 M KOH to ensure reproducibility before testing, with standard deviations for voltage and power density of <±0.013 V and <±0.006 mW cm^{-2} recorded respectively (Appendix A: Fig. A1).

2.2. Solution and material analysis

Solution conductivity and pH was determined off-line (Seven2Go Pro S7, Mettler Toledo, Leicester, UK; 4330, Jenway, Stone, UK). COD and ammoniacal nitrogen concentrations were measured using standard spectrophotometric cell test kits (11451 COD, 114,559 NH₄⁺-N, Spectroquant® cell tests, Merck Millipore, Watford, UK). Ammoniacal nitrogen measurement involved sample acidification to convert all ammoniacal nitrogen to ammonium giving a concentration as NH₄⁺-N for the total ammoniacal nitrogen content. Soluble COD (sCOD) was measured after filtration through 0.45 μm filter (Merck Millipore, UK). Ultraviolet sample absorbance (UV$_{254nm}$) was determined using UV–vis spectrophotometry (6715, Jenway, Cole Parmer, UK). Membrane and electrode samples were dried before characterisation by fourier
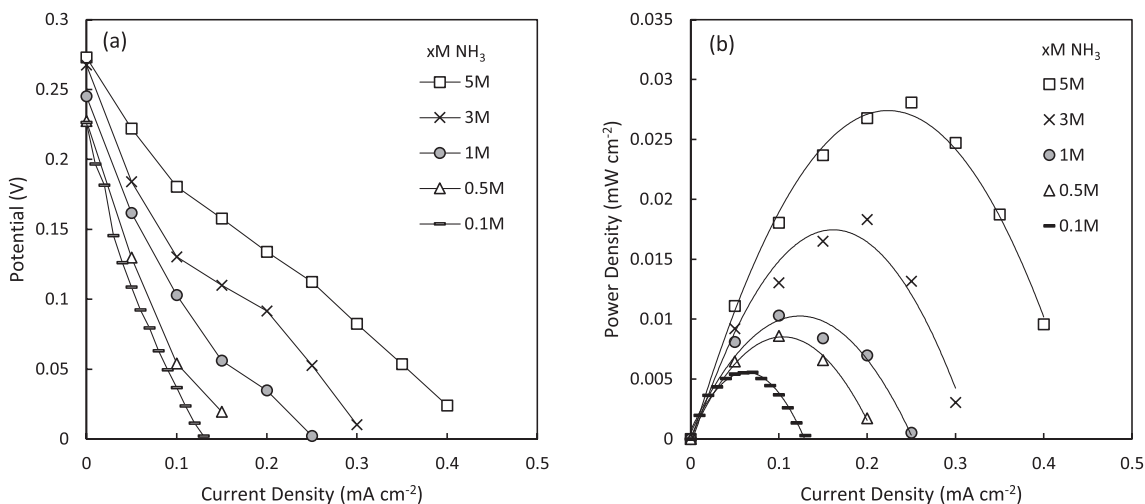
Fig. 5. Polarisation curves for pure synthetic solutions of ammonia of different concentrations (a) potential and (b) current density.
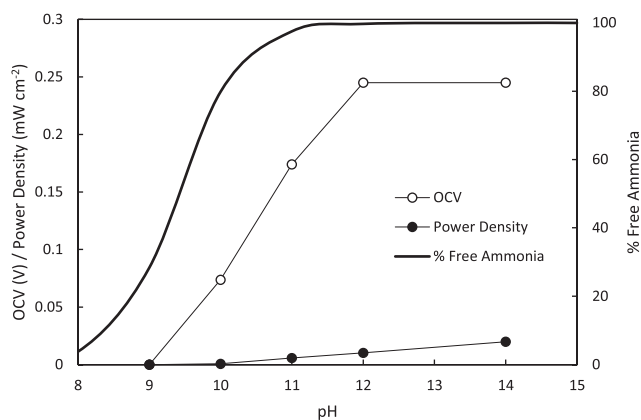

Fig. 6. Impact of solution pH on fuel cell performance showing the OCV, power density and % free ammonia in solution for a synthetic 1 M NH_3 feed at 40 °C.

transform infrared (FTIR) spectroscopy (Vertex 70, Bruker, UK) to discern competitive adsorption/deposition of trace contaminants. Total solids and total suspended solids were measured using standard methods 2540B and 2540D (APHA/AWWA/WEF, 2012). Solution surface tension was measured using a ring tensiometer (K6 Force Tensiometer, Kruss, GmbH, Bristol, UK).

2.3. Chemicals and wastewater sampling

Ammonium hydroxide (35%, Fisher, UK) and potassium hydroxide (85% flake, Alfa Aesar, UK) were used to produce synthetic ammonia solutions for initial fuel cell characterisation. Where required, pH was adjusted using sulphuric acid (95%, Alfa Aesar, UK) or potassium hydroxide. Deionised water with a resistivity of 15 MΩ cm was used throughout (Purelab Option ELGA, Veolia, UK). Municipal centrate (liquid fraction of digested sludge) was collected from the return liquor line of an advanced anaerobic digestion (AD) plant at a local sewage treatment works and stored <5 °C before use.

3. Results and discussion

3.1. Vacuum thermal stripping produces a concentrated aqueous solution suitable for fuel cells

Ammonia recovery from real municipal centrate (return liquor) was undertaken in batch with vacuum thermal stripping (Fig. 3). The

centrate ammonia concentration was 0.12 M (2.01 gNH$_3$ L^{-1}) which is typical of an advanced AD [29]. An initial pH of 8 and conductivity of 14.6 mS cm^{-1} was recorded (Table 2). Within 0.2 h, 24% of the feed ammonia fraction was transferred to the gas phase, which is sufficient to create an aqueous distillate with an ammonia concentration of 3.4 M, equivalent to a concentration factor (based on the initial feed concentration) of 27.9 (Fig. 3). As the batch cycle continued, the rate of ammonia transfer declined. This can be explained by the transition across the vapour liquid equilibrium that occurs with the decline in feed concentration, as the reduction in vapour pressure of the feed, lowers the ammonia fraction that can develop in the vapour phase (Fig. 4, constructed using the approach of Pátek and Klomfar [30]). Consequently, the distillate was diluted and a final concentration of 17.3 gNH$_3$ L^{-1} (1 M) was achieved, representing a concentration factor of 8.7. At full scale, vapour pressure could be controlled by dynamically adjusting vacuum pressure to sustain an operating point at a fixed position within the vapour liquid equilibrium (VLE), to create a consistent vapour phase concentration during the batch cycle to improve final aqueous product concentration [14]. Importantly, >85% ammonia separation was achieved during the fixed 1.5 h batch cycle, leading to the production of a transparent aqueous ammonia distillate, as indicated by a reduction in UV$_{254nm}$ transmission (Fig. B2, Table 2). The conductivity of the distillate (26.2 mS cm^{-1}) is considerably higher than the conductivity of a synthetic ammonia solution of comparable concentration (1.2 mS cm^{-1}; Table 2). This may be due to the co-transport of low MW VOCs that can strongly influence solution conductivity [31]. However, the COD concentration was 248 mg L^{-1} which is equivalent to a 96% reduction when compared to the centrate (5773 mg L^{-1}). While organic compounds have been indicated to introduce electrode contamination into DAFC which could lower fuel cell efficiency and been shown to lead to a reduction in both OCV and power density [7,8], it is the chemistry and not just the concentration which is important as vacuum stripping is not selective for higher MW organics (e.g., proteins and exopolysaccharides) conventionally associated with membrane and electrode fouling. Significantly, the ammonia concentration and natural pH of the distillate (10.5) are conducive to application within a DAFC [20].

3.2. Impact of distillate solution chemistry on power generation from a direct ammonia fuel cell

The impact of distillate chemistry on power generation from DAFC was initially conducted using synthetic aqueous ammonia to provide a baseline for cell performance. Ammonia concentrations between 0.1 and 5 M were studied which is a range which can be practically achieved with thermal stripping [14]. Open Circuit Voltage (OCV), which is the
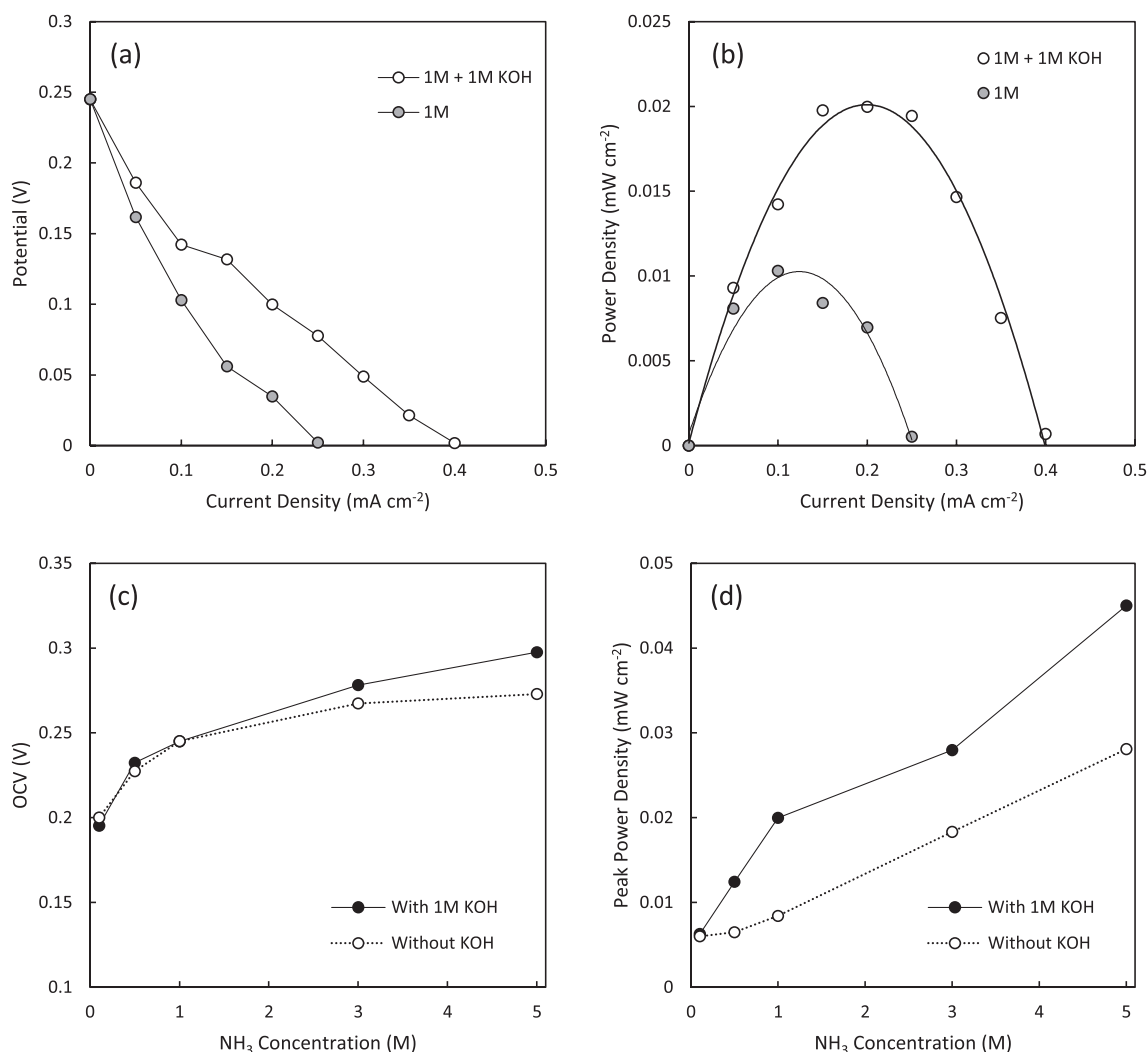
Fig. 7. Performance of the direct ammonia fuel cell with synthetic solutions of ammonia or ammonia with 1 M potassium hydroxide (a) polarisation curves, (b) power density, (c) open circuit voltage and (d) peak power density (all solutions at natural pH (11.15–12.58), temperature = 40 °C).

voltage observed when no current is flowing (Fig. 5a, current density 0 mA cm^{-2}), improved from 0.22 to 0.27 V as ammonia concentration was increased, and is comparable to previous observations [7,26]. However, OCV is considerably below the theoretical potential (1.17 V, Eq. (1)) calculated from the half reactions at the anode and cathode (Eqs. (2) and (3)). This can be observed for DAFC due to cell inefficiencies such as ammonia cross-over through the AEM, activation polarisation or concentration polarisation [19]. Power density increased by ~400% when ammonia concentration increased from 0.1 to 5 M due to the greater quantity of ammonia available for oxidation at the anode [26] (Fig. 5b). Due to the high adsorption energy of N to the Pt electrocatalyst, future study establishing robustness to longer term operation would be beneficial [27]. The power densities obtained with DAFC using AEM is rather lower compared to the power densities obtained with SOFCs, which is attributed to the low catalytic activity of the electrode materials at ambient operating temperature in DAFC [12]. However, considerable optimisation of the DAFC can be achieved through detailed componential characterisation with a conventional three-electrode system before practical implementation of the technology.

The pH of the recovered distillate (10.5) was below that of a synthetic ammonia solution of equivalent concentration (11.8), which could be explained by the co-separation of organic acids reducing the basicity of the ammonia solution (Table 2). As pH is reduced, a higher proportion of ammonia becomes protonated to form ammonium

(NH$_4^+$), lowering the NH$_3$ fraction available for oxidation [32] (Fig. 6). Consequently, the cell OCV increases as free ammonia concentration is increased by raising solution pH, until pH12 where a plateau was achieved due to the complete deprotonation of ammonia. Within the lower pH range, OCV reduced to 0 V at pH9 despite a free ammonia fraction of 28% remaining [32]. This can be explained by the addition of [H$^+$] which is inversely proportional to the [OH$^-$] concentration. Sufficient [OH$^-$] must be present at the anode to facilitate ammonia oxidation (Eq. (2)) [19]. The reduction in power density is therefore due to the reduction in free ammonia and [OH$^-$] in solution due to pH dependent equilibria, but may also reflect membrane transport properties, where a thinner membrane (450 μm in this study, Table 1) comprising optimum structural and morphological properties could better mediate [OH$^-$] transport from the cathode [33]. The significance of [OH$^-$] transport limitation to power generation was further investigated by supplementing synthetic solution with a natural pH of 11.8, where ammonia is almost completely deprotonated, with a potassium hydroxide (KOH) solution raising pH to 14 providing a greater excess of [OH$^-$] (Appendix A: Fig. A2, Table A1). Addition of 1 M KOH improved potential across the cell, approximately doubling power density by improving ammonia oxidation efficiency at the anode (Fig. 7b). However, the relatively small impact of KOH addition on OCV confirms that the electrical potential is mainly associated with ammonia (Fig. 7c) [7]. At low ammonia concentrations (<1M), an excess of [OH$^-$] is less significant to improving
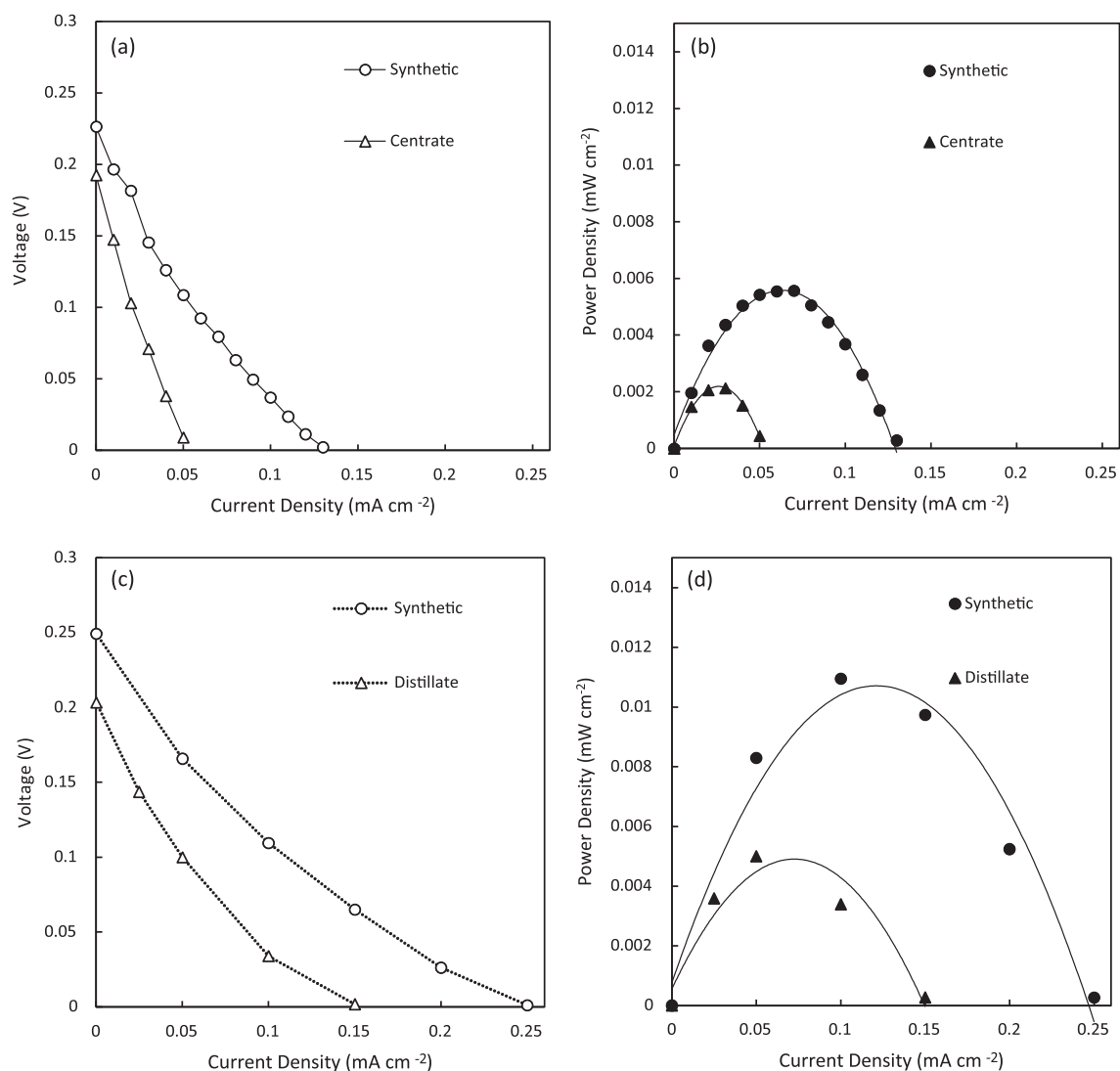
Fig. 8. Performance of the direct ammonia fuel cell with either wastewater derived ammonia solutions or pure ammonia solution; (a) polarisation curve and (b) power density of wastewater centrate and a synthetic ammonia solution of an equivalent ammonia concentration (~0.12 M); (c) polarisation curve and (d) power density of recovered distillate and pure synthetic ammonia solution at an equivalent ammonia concentration (~1M). (All solutions at natural pH, temperature = 40 °C).

power density but as ammonia concentration increases above 1 M, the relative efficiency gain is considerable and consistent, improving power density by around 200% as ammonia concentration is increased (Fig. 7d and C). This consistency in power density increase is ascribed to the increased [OH⁻] concentration that compensates for mass transfer limitation in the cell design. Consequently, while addition of [OH⁻] may be advantageous to energy generation, the need for supplemental [OH⁻] can be reduced by improving [OH⁻] transport through better cell design, such as the development of AEMs with improved [OH⁻] conductivity [31].

3.3. Power generation from ammonia distillate is considerably greater than from direct centrate

Energy generation from ammonia using the DAFC was performed with wastewater centrate from a return liquor as well as with the thermally recovered distillate to confirm the advantage of thermal separation in the concentration and purification of ammonia from centrate (Fig. 8). An OCV of 0.19 V was recorded for the wastewater centrate, which is higher than would be expected as the centrate pH was below the minimum required to exhibit a cell potential with deprotonated

ammonia (Fig. 6) and was broadly comparable to a synthetic ammonia solution of comparative concentration. Zhang *et al.* [7] reported a power density of 0.08 mW cm^{-2} from ammonia rich landfill leachate compared to 0.11 mW cm^{-2} for synthetic solution, and while the pH was not reported, landfill leachate is typically between pH 4.5 and 9 [34] which would limit availability of deprotonated ammonia for oxidation at the anode. We therefore propose that the favourable power density achieved is due to competitive oxidation of organics, as energy generation from short chain alcohols [35,36], sugars [36] and urea (an amide containing carbon and nitrogen) [8] commonly present in wastewater [30] have been independently verified with alkaline fuel cells. Analysis of the AEM by FTIR following exposure to centrate indicated absorbance at 3363 cm^{-1} (Fig. 9) which confirmed the presence of compounds containing alcohol and primary amine functional groups which readily undergo electrochemical oxidation (Table 3) [8,36,37]. In this study, FTIR was used to identify the types of organic compounds that might influence fuel cell operation; having narrowed the explicit associative chemistries, analytical techniques (e.g. GC–MS; HPLC) can now be used to link organic concentration to implications for fuel cell resilience.

The OCV of 0.2 V obtained with aqueous ammonia distillate (Fig. 7) was comparable to the centrate but the ratio of ammonia to COD
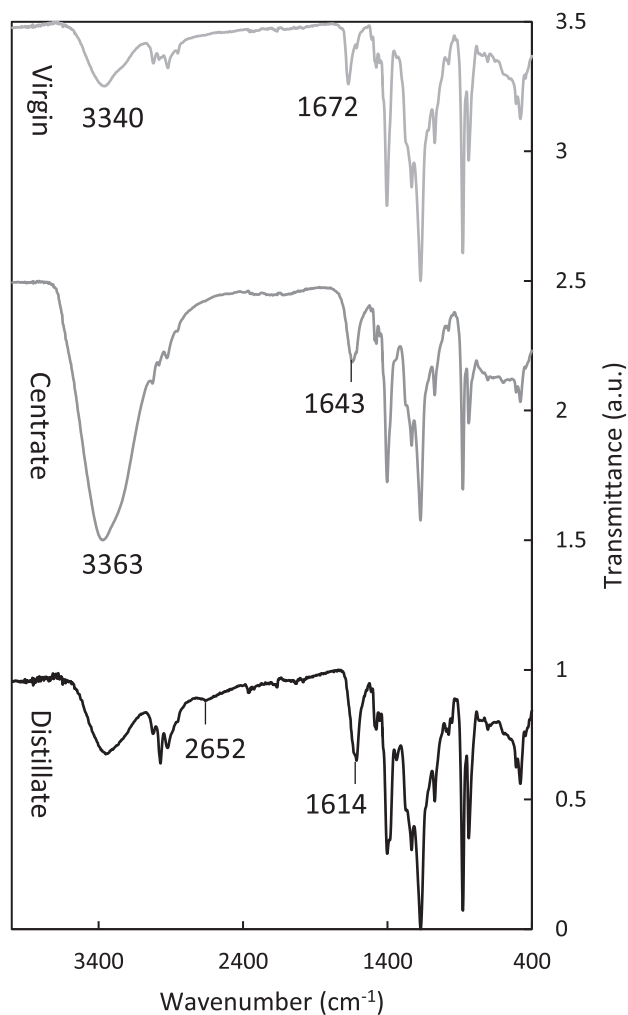
Fig. 9. FTIR analysis of the anion exchange membrane used in fuel cell analysis showing the virgin membrane, membrane applied with centrate and membrane applied with distillate.

Table 3
Infrared absorbances for various functional groups observed in FTIR of the anion exchange membranes [37].

Bonds	Molecules	Peak position (cm^{-1})
O—H, N—H	Alcohols, Amines (primary), Amides (primary/ secondary)	3500–3000
N—H	Amines (secondary/tertiary)	2700–2300
C=O	Amides	1695–1630

concentration was 200 times higher (NH_3/COD, 69.8 and 0.35 respectively), emphasising that the electrochemical potential of the distillate was primarily associated with the ammonia fraction (Table 2). The power density of 0.005 mW cm^{-2} recorded for the distillate was 2.5 times higher than recorded from wastewater centrate (0.002 mW cm^{-2}). Consequently, by concentrating ammonia, vacuum thermal stripping can increase power output, lowering investment cost for fuel cell technology. However, distillate power density was lower than observed with synthetic aqueous ammonia of comparable concentration, which we propose is due to the lower pH (10.5). Bavarella et al. [14] produced a 6.4 M aqueous product with a natural pH of 11.5, which we suggest is due to the basicity provided by the higher ammonia concentration compensating for the acidity of the small fraction of co-transported VOCs. Therefore, by transitioning to an optimum operating point in

the vapour-liquid-equilibrium, a pH comparable to synthetic ammonia solution can be achieved, increasing ammonia oxidation at the anode (Fig. 6) [19] and will be complemented by a higher power density due to the increased ammonia concentration. While a comparatively negligible organic fraction was present in the distillate produced from centrate, deposition of VOC like compounds was confirmed by FTIR, where a shift in absorbance at 1672 cm^{-1} in the virgin membrane to 1614 cm^{-1} in the AEM exposed to distillate, is attributed to various —C=O stretches of carbonyl groups associated with a group of low MW volatile organic carbonyls identified in sewage (Fig. 9, Table 3) [28,37]. Although several mechanistic pathways likely exist in which this organic fraction may interfere with fuel cell performance, particular components such as the gas diffusion layer of the membrane electrode assembly is known to be particularly sensitive to changes in surface tension [38]. It is likely therefore that the reduced surface tension of the ammonia distillate (Table 2) will adversely impact the performance of this component of the DAFC particularly during long term application. Longer-term studies seeking to establish implications of deposition on material integrity of each fuel cell component are therefore warranted.

3.4. Ammonia concentration is critical to synergising thermal recovery with energy recovery

This work has demonstrated the potential to recover concentrated ammonia from wastewater with electrical energy produced from the purified product. Thermal analysis was undertaken to characterise the energy demand required for vacuum stripping based on the operating conditions used (65 °C, 0.25 bar(a)), to produce the 1.1 M aqueous ammonia product (Fig. 10, Appendix B). The analysis determines sensible and latent heat demand for separation, together with heat recovered through condenser and heat exchanger design, which results in a net separation energy demand of 44 kWh kgN^{-1} (0.65 kW h kg N^{-1} for vacuum). For reference, the aeration energy requirement for ammonia removal is 6 kW h kg N^{-1} [3], indicating a considerably higher energy demand for thermal separation than biological treatment (following centrate return to head of works). However, the unit cost for heat is considerably cheaper than electricity. Consequently, the unit cost difference between aeration and thermal separation for ammonia removal begin to converge (£0.78 kg N^{-1} and £1.32 kg N^{-1}, respectively). As the fuel cell used for this study was not a complete stack, electrical energy production from ammonia was based on fuel cell conversion efficiency from the literature (60%) [39,40] resulting in 6.7 kW h m^{-3} centrate or 3.76 kW h kg N^{-1} removed. Factoring in the electrical energy from ammonia, the cost of ammonia removal reduces to £0.62 kg N^{-1}, making thermal ammonia separation cost competitive to conventional treatment.

The direct cost for heat can be significantly reduced through two routes: using waste heat from AD facilities co-located with centrate separators, and by reducing the latent heat penalty for water transport. There is an estimated 42 kW h$_{th}$ m^{-3} of centrate with sufficient heat quality (85 °C) [41] to lower thermal demand by 6.25 kW h$_{th}$ kg N^{-1}, reducing net cost to £0.43 kg N^{-1}. Alternatively, there is also the potential to improve the DAFC performance by increasing the feed temperature [42], but further investigation is needed of the integrated system to establish how best to value the exploitation of waste heat considering the trade-off between its use for thermal ammonia separation or for driving improved power output from the DAFC system. In this study, the vacuum pressure was operated in an open mode (unmodulated) where the vapour pressure subsequently defers to the dew point (final boiling point) of the two-phase mixture. This is comparable to the existing literature on vacuum ammonia strippers [15,43] and results in a relatively dilute final product due to the significant co-transport of water vapour (Appendix B: Fig. B1). The primary heat demand for separation is the latent heat penalty for water [14]. We propose that water vapour transport can be dissipated by modulating vacuum pressure to operate below the dew point to reduce the energy demand for separation (<16
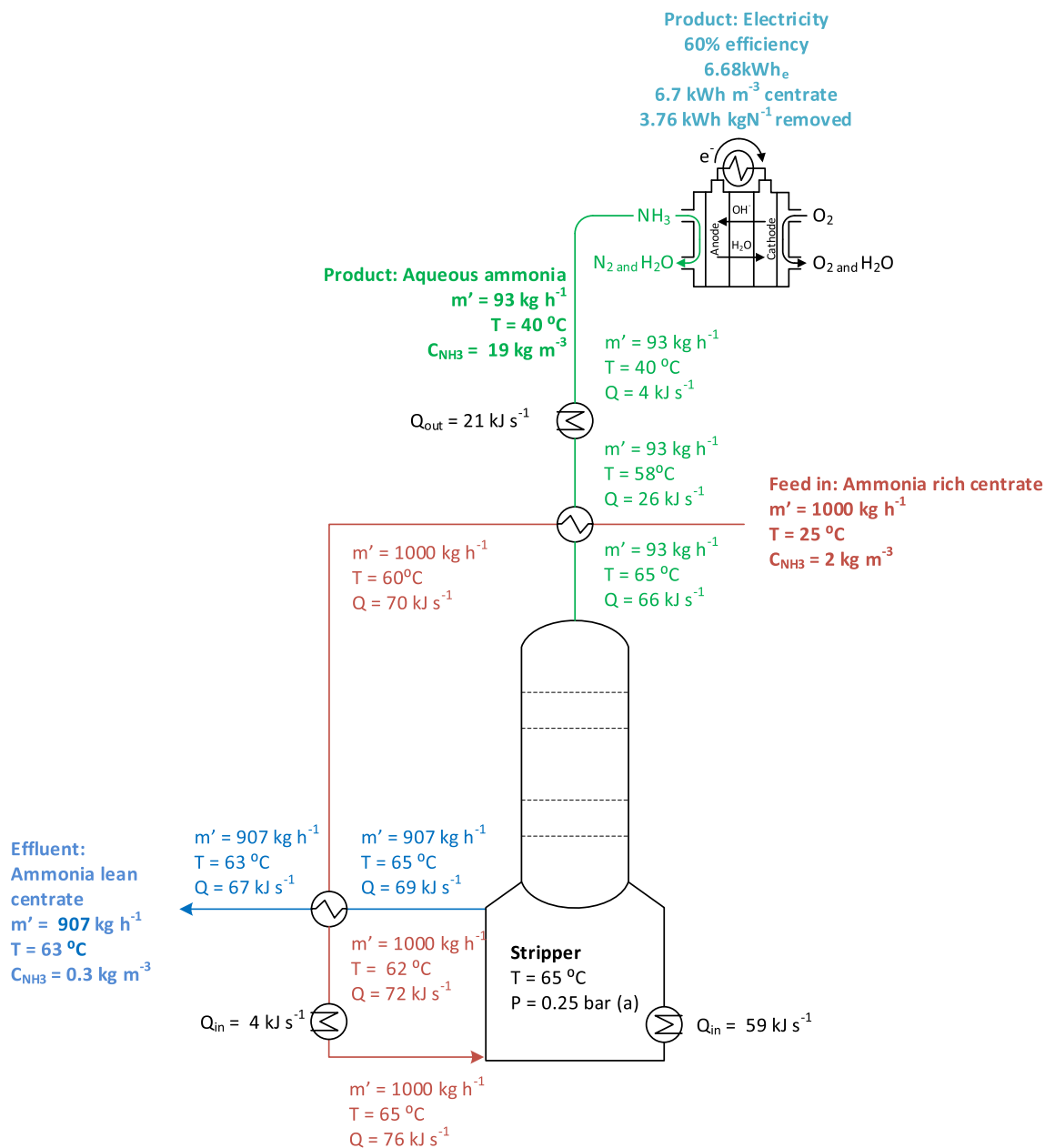
Fig. 10. Mass and energy balance for ammonia recovery from centrate based on separation achieved using vacuum thermal stripping (85% removal; 19 kg m^{-3} (1.1 M) aqueous ammonia produced; T 65 °C, P 0.25 bar(a)).

kW h kgN^{-1}) and create a more concentrated ammonia product, improving fuel cell power density (Fig. 5), therefore providing a significant reduction in capital cost. Carbon emissions of −8.1 kg CO$_2$ kg N^{-1} are directly associated with heat demand for thermal stripping. This can be reduced by switching from extrinsic fossil sources to biogas or waste heat (Table 4). However, with carbon savings provided through the avoidance of N$_2$O emissions by thermal stripping, together with carbon offset through electricity production from aqueous ammonia, it is sufficient to create a net positive carbon position (+3.67 kg CO$_2$ kg N^{-1}) even with the use of fossil derived heat and illustrates the net zero credentials of switching to production of this carbon free ammonia fuel.

4. Conclusions

This study has demonstrated the transformation of ammonia from real wastewater into a carbon free fuel using vacuum stripping to separate and concentrate ammonia before fuel cell application to improve energy generation:

● Ammonia distillate concentration is dependent upon the vapour pressure applied. The reduction in vapour pressure in a binary distillation system (water-ammonia) reduces selectivity for ammonia. Improved characterisation of the ammonia-water vapour-liquid-equilibrium will enable closer control of final product quality.

Table 4

Impact of thermal ammonia recovery on cost and carbon.

Parameter	Baseline scenario compared to thermal ammonia recovery using imported gas						Thermal ammonia recovery with waste heat based on same operating point		
	Energy (kW h kgN^{-1})	Unit cost (£ kW h^{-1})	Net cost (£ kgN^{-1})	Emissions factor		Net emissions (kg CO$_2$ kgN^{-1})	Energy (kW h kg N^{-1})	Net cost (£)	Net emissions (kg CO$_2$ kg N^{-1})
Aeration energy demand	6	0.13	−0.78	0.233[a]	kgCO$_2$ kW h^{-1}	−1.40	6	−0.78	−1.40
N$_2$O emissions	–	–	–	0.035[b]	kg N$_2$O kg N^{-1}	+10.43[d]	–	–	+10.43[d]
Thermal energy demand	44	0.03	−1.32	0.184[a]	kg CO$_2$ kW h^{-1}	−8.10	37.75	−1.13	−6.95
Vacuum energy demand	0.65	0.13	−0.08	0.233[a]	kg CO$_2$ kW h^{-1}	−0.15	0.65	−0.08	−0.15
Energy from ammonia	6.4[c]	0.13	+0.78	0.233[a]	kg CO$_2$ kW h^{-1}	+1.49	6.4	+0.78	+1.49
Net energy cost/ carbon			*−0.62*			*+3.67*		*−0.43*	*+4.82*

Fuel cell efficiency 60% [39,40].

[e] Waste heat addition 2.5 kW h m^{-3} (6.25 kW h kg N^{-1}) [41].

[a] Bulb.co.uk/carbon-tracker.

[b] Foley and Lant [44].

[d] 298 kg CO$_2$ kg N$_2$O^{-1}.

- The co-transport of low MW volatile organic compounds reduced distillate pH, which limited fuel cell power density as pH governs the deprotonation of ammonia needed to promote oxidation at the anode. The lower pH also reduced [OH$^-$] availability for electrochemical conversion.
- While the fuel cell in this study was used as a reference to discriminate the effect of discrete fuel properties on performance, [OH$^-$] limitation also highlighted the critical role of the membrane transport properties in mediating fast and efficient [OH$^-$] transport from the cathode. However, this should be complemented by an increase in ammonia concentration of the product to achieve economic power densities.
- Vacuum stripping can produce a consistent concentrated ammonia product of considerably higher purity than the original solution, including a significant reduction in the organic fraction. However, the low MW carbonyl compounds identified may have long-term implications for fuel cell stability. This requires further study to identify the long-term risk of VOCs on fuel cell performance, that may indicated the need for pretreatment.
- The high thermal demand for ammonia vacuum stripping is primarily due to the simultaneous vaporisation of water (latent fraction) with ammonia. While further work is required, we propose that by reducing the operating point from the dew point (conventional vacuum stripping) toward the bubble point (with in the two-phase region of the vapour-liquid equilibrium), the vaporisation of water can be largely reduced to yield a concentrated ammonia product, and requiring less separation energy, which drives a synergistic improvement in fuel cell efficiency.
- Despite the heat demand for the ammonia produced in this study (1 M), the cost of heat coupled with the power production from ammonia indicate a favourable economic return, which can be further improved through the use of waste heat, biogas and a reduction in heat demand. From the carbon balance, it is also evidenced that by revaluing ammonia as a carbon free fuel, wastewater treatment can be repositioned for a carbon positive future.

CRediT authorship contribution statement

C.J. Davey: Conceptualization, Data curation, Formal analysis, Funding acquisition, Investigation, Methodology, Project administration, Resources, Writing – original draft. **B. Luqmani:** Data curation, Formal analysis, Investigation, Methodology, Writing – review & editing. **N. Thomas:** Data curation, Methodology, Writing – review & editing. **E.J. McAdam:** Conceptualization, Data curation, Funding acquisition, Project administration, Resources, Writing – review & editing.

Declaration of Competing Interest

The authors declare that they have no known competing financial interests or personal relationships that could have appeared to influence the work reported in this paper.

Acknowledgements

Appendix A:. Fuel cell data to evidence replication and the implications of additive [OH$^-$]

Fig. A1 evidences quality assurance through a triplicate of polarisation curves, with error bars plotted as standard deviation of the triplicate. Fig. A2 and Table A1 provide supporting polarisation curves for experiments with supplemental KOH at each ammonia concentration (Fig. 8), including demonstrating the impact of KOH addition on solution pH (Table A1).
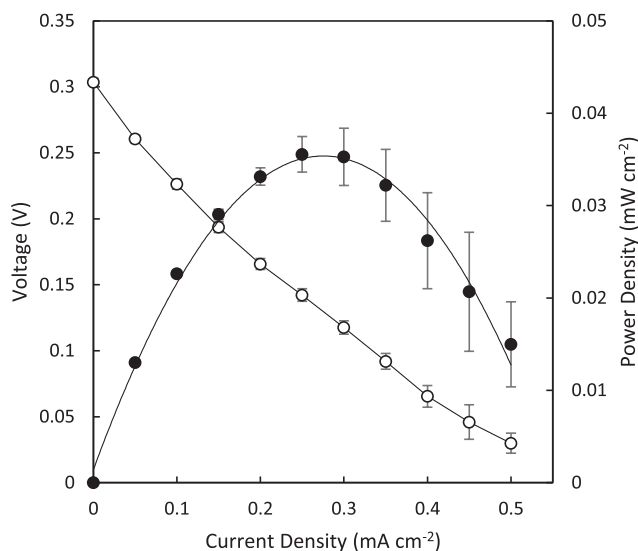
Fig. A1. Polarisation curve and power density data from the average of three separate fuel cells for a solution of 5 M NH_3 and 1 M KOH. Error bars show standard deviation between these three data sets.
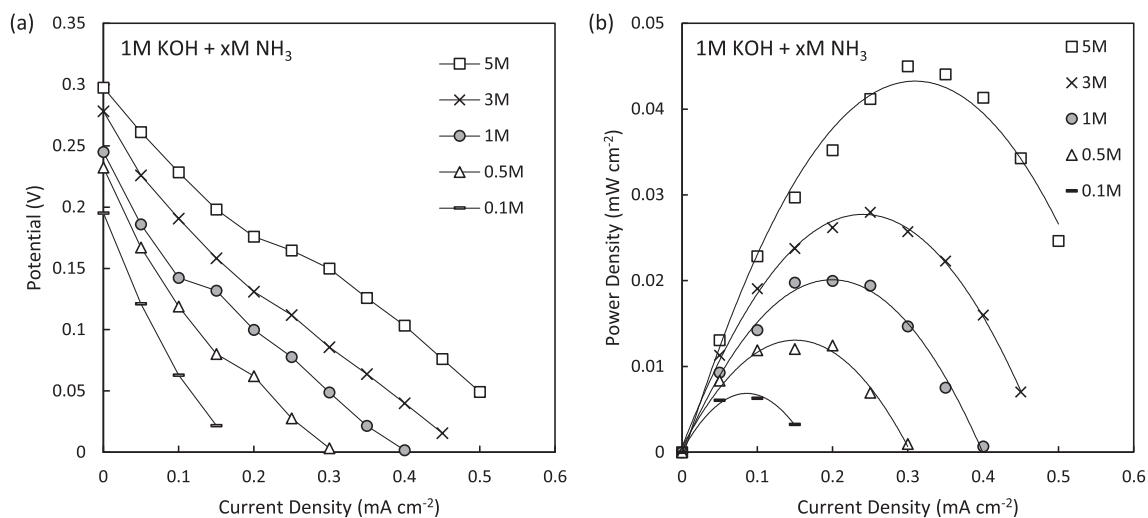

Fig. A2. Full (a) polarisation curves and (b) power density data for synthetic ammonia solutions with addition of 1 M KOH (all solutions at natural pH, temperature = 40 °C).

Table A1

Conductivity and pH of the synthetic ammonia solution with and without addition of 1 M KOH.

Ammonia concentration (M)	Conductivity (mS cm^{-1})		pH	
	$xM\ NH_3$	$xM\ NH_3 + 1\ M\ KOH$	$xM\ NH_3$	$xM\ NH_3 + 1\ M\ KOH$
0.1	0.4	185	11.15	14.25
0.5	0.8	186	11.66	14.31
1	1.2	186	11.83	14.43
3	1.36	170	12.24	14.52
5	1.6	154	12.58	14.65

Appendix B:. Ammonia stripper mass and energy balance

A mass balance was conducted across the vacuum stripper to calculate the mass flow and composition of the four major process streams (Table B1) based on the centrate evaluated (2 kg N m^{-3}) and condensate produced following experiments (9% water vaporisation; 86% ammonia separation, Fig. B1) which yielded a transparent distillate (Fig. B2). To normalise data, an inlet flowrate of 1000 kg h^{-1} was assumed, and from this a mass balance was created (Table B1). The sensible heat required to raise centrate feed temperature was calculated (B1):

$$Q'_{sensible} = m' C_p \Delta T \tag{B1}$$

Table B1

Ammonia stripper mass balance overview.

Parameter		Process stream			
		Centrate in	*Centrate out*	*Vapour out*	*Distillate out*
Total flow	kg h^{-1}	1000	907	93	93
NH$_3$ flow	kg s^{-1}	0.0006	0.0001	0.0005	0.0005
H$_2$0 flow	kg s^{-1}	0.28	0.25	0.03	0.03
NH$_3$ fraction	(by mass)	0.0020	0.0003	0.0185	0.0185
H$_2$0 fraction	(by mass)	0.9980	0.9997	0.9815	0.9815
NH$_3$ conc.	kg m^{-3}	2.0	0.3	–	18.9

Operating point
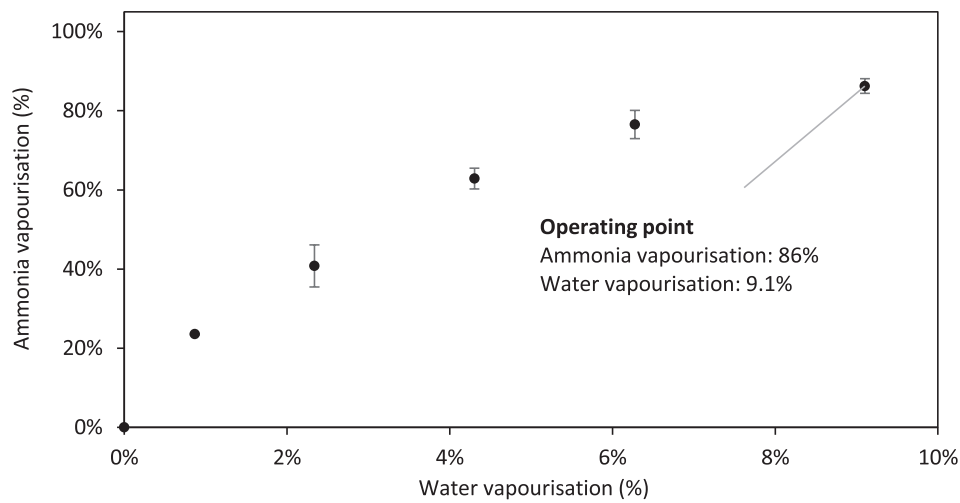Ammonia vapourisation: 86%
Water vapourisation: 9.1%

Fig. B1. Vaporisation of water and ammonia during ammonia stripping (65 °C; 0.25 bar(a)).

Fig. B2. Photo of wastewater centrate from an advanced anaerobic digester (left) and recovered ammonia distillate (right).

Table B2

Input conditions for ammonia stripper energy balance.

Parameter		
Centrate in: Temperature	25	°C
Stripper: Operating temperature	65	°C
Vapour out: Bubble temperature, T_b[a]	58	°C
Vapour out: Dew temperature, T_d[a]	40	°C
Heat exchanger: Approach temperature, T_{app}[b]	3	°C
Water: Enthalpy of vapourisation (65C), ΔH_v[c]	2345	kg kJ^{-1}
Water: Specific heat capacity, C_p[d]	4.2	kJ kg^{-1} C^{-1}

[a] Calculated using empirical function [30] and vapour composition (Table 2).
[b] Design value based on reasonable minimum [45].
[c] [46].
[d] [46].

where $Q'_{sensible}$ represents sensible energy flow (kJ s^{-1}), m' is mass flow (kg s^{-1}), C_p is isobaric specific heat capacity (kJ kg^{-1} °C^{-1}), and ΔH_v is the enthalpy of vapourisation (kJ kg^{-1}). The latent heat required to vaporise the water fraction was calculated based on the enthalpy of vapourisation (B2).

$$Q'_{latent} = m' \Delta H_v \tag{B2}$$

where Q'_{latent} represents latent energy flow (kJ s^{-1}). The cooling required to condense the vapour stream to the dewpoint was calculated (Eqs. B(1) and B(2)) based on the vapour flow, dewpoint temperature and enthalpy of vaporisation (Table B2). A counter-current heat exchanger was designed to pre-heat the incoming centrate using the vapour stream exiting the ammonia stripper. This was simplified by assuming that the vapour would be cooled from its superheated state to its bubble temperature to avoid considerations of latent energy exchange during partial condensation. The outstanding cooling duty required to cool and condense the vapour stream was calculated (Eqs. B(1) and B(2), Table B1 and B2) and assigned to a combined cooler and total condenser to produce the final distillate. The available sensible heat was calculated and assumed to transfer into the centrate feed with zero losses. A second countercurrent heat exchanger was designed to pre-heat the centrate using the centrate stream exiting the ammonia stripper. An approach temperature (Table B2) was applied to limit heat transfer across streams. The maximum available sensible heat was calculated and assumed to transfer into the centrate feed with zero losses. Following heat integration, the remaining sensible heat required for the centrate was calculated and assigned to a final supplementary heat exchanger.

The electrical energy required for the vacuum, was estimated using a liquid ring vacuum pump (which can match the pressure and flowrates required for this application) [47]:

$$P_{is} = P_a . S \frac{P_e}{P_a} \tag{B3}$$

where P_{is} is the isothermal compression power for the pump (kW); P_a is the suction pressure (kPa); P_e is the compression pressure (101.25 kPa); P_a is the suction pressure (kPa). S (the air equivalent suction flowrate, m^3 s^{-1}) can be determined by:

$$S = \frac{G}{\rho_{air}} \sqrt{\frac{T_v MW_v}{T^0 MW_{air}}} \tag{B4}$$

where G is the vapour flowrate (kg s^{-1}); T_v is the vapour temperature (K); T^o is the outlet temperature (293.15 K); MW_v is the molecular weight for vapour (kg kmol^{-1}) and MW_{air} is the molecular weight for air (28.96 kg kmol^{-1}).

References

[1] B. Wett, Solved upscaling problems for implementing deammonification of rejection water, Water Sci. Technol. 53 (12) (2006) 121–128.

[2] DEFRA (Department for Environment Food & Rural Affair), Clean air strategy 2019, 2019.

[3] Enerwater, D4.5 ENERWATER Actual Energy Savings Evaluation Report, 2018.

[4] R. Lan, S. Tao, Ammonia as a suitable fuel for fuel cells, Front. Energy Res. 2 (2014) 3–6.

[5] POST (Parliamentary Office of Science and Technology), Energy and sewage, Postnote number 282, 2007.

[6] N. van Linden, Y. Wang, E. Sudhölter, H. Spanjers, J.B. van Lier, Selectivity of vacuum ammonia stripping using porous gas-permeable and dense pervaporation membranes under various hydraulic conditions and feed water compositions, J. Membr. Sci. 642 (2022) 120005, https://doi.org/10.1016/j.memsci.2021.120005.

[7] M. Zhang, P. Zou, G. Jeerh, S. Chen, J. Shields, H. Wang, S. Tao, Electricity generation from ammonia in landfill leachate by an alkaline membrane fuel cell based on precious-metal-free electrodes, ACS Sustain. Chem. Eng. 8 (34) (2020) 12817–12824.

[8] G. Gnana kumar, A. Farithkhan, A. Manthiram, Direct Urea Fuel Cells: Recent progress and critical challenges of urea oxidation electrocatalysis, Adv. Energy Sustain. Res. 1 (2020) 2000015.

[9] S. Heile, C.A.L. Chernicharo, E.M.F. Brandt, E.J. McAdam, Dissolved gas separation for engineered anaerobic wastewater systems, Sep. Purif. Technol. 189 (2017) 405–418.

[10] A.J. Ward, K. Arola, E. Thompson Brewster, C.M. Mehta, D.J. Batstone, Nutrient recovery from wastewater through pilot scale electrodialysis, Water Res. 135 (2018) 57–65.

[11] H. Cruz, Y.Y. Law, J.S. Guest, K. Rabaey, D. Batstone, B. Laycock, W. Verstraete, I. Pikaar, Mainstream ammonium recovery to advance sustainable urban wastewater management, Environ. Sci. Technol. 53 (2019) 11066–11079.

[12] R. Lan, S. Tao, Direct ammonia alkaline anion-exchange membrane fuel cells, Electrochem. Solid-State Lett. 13 (8) (2010) B83, https://doi.org/10.1149/1.3428469.

[13] B. Teichgräber, A. Stein, Nitrogen elimination from sludge treatment reject water – comparison of the steam-stripping and denitrification processes, Water Sci. Technol. 30 (6) (1994) 41–51.

[14] S. Bavarella, M. Hermassi, A. Brookes, A. Moore, P. Vale, I.S. Moon, M. Pidou, E. J. McAdam, Recovery and concentration of ammonia from return liquor to promote enhanced CO2 absorption and simultaneous ammonium bicarbonate crystallisation during biogas upgrading in a hollow fibre membrane contactor, Sep. Purif. Technol. 241 (2020) 116631.

[15] A.T. Ukwuani, W. Tao, Developing a vacuum thermal stripping–acid absorption process for ammonia recovery from anaerobic digester effluent, Water Res. 106 (2016) 108–115.

[16] B. Stoeckl, M. Preininger, V. Subotić, S. Megel, C. Folgner, C. Hochenauer, Towards a wastewater energy recovery system: The utilization of humidified ammonia by a solid oxide fuel cell stack, J. Power Sources 450 (2020) 227608.

[17] N. van Linden, H. Spanjers, J.B. van Lier, Fuelling a solid oxide fuel cell with ammonia recovered from water by vacuum membrane stripping, Chem. Eng. J. 428 (2022) 131081.

[18] Y. Zhao, B.P. Setzler, J. Wang, J. Nash, T. Wang, B. Xu, Y. Yan, An efficient direct ammonia fuel cell for affordable carbon-neutral transportation, Joule 3 (10) (2019) 2472–2484.

[19] N.V. Rees, R.G. Compton, Carbon-free energy: a review of ammonia- and hydrazine-based electrochemical fuel cells, Energy Environ. Sci. 4 (2011) 1255–1260.

[20] G. Jeerh, M. Zhang, S. Tao, Recent progress in ammonia fuel cells and their potential applications, J. Mater. Chem. A 9 (2) (2021) 727–752.

[21] R. Chen, S. Zheng, Y. Yao, Z. Lin, W. Ouyang, L. Zhuo, Z. Wang, Performance of direct ammonia fuel cell with PtIr/C, PtRu/C, and Pt/C as anode electrocatalysts under mild conditions, Int. J. Hydrog. Energy 46 (54) (2021) 27749–27757.

[22] P. Zou, S. Chen, R. Lan, S. Tao, Investigation of perovskite oxide SrCo0.8Cu0.1Nb0.1O3–Δ as a cathode material for room temperature direct ammonia fuel cells, ChemSusChem 12 (12) (2019) 2788–2794.

[23] F.J. Vidal-Iglesias, J. Solla-Gullón, V. Montiel, J.M. Feliu, A. Aldaz, Screening of electrocatalysts for direct ammonia fuel cell: ammonia oxidation on PtMe (Me: Ir, Rh, Pd, Ru) and preferentially oriented Pt(100) nanoparticles, J. Power Sour. 171 (2007) 448–456.

[24] P. Zou, S. Chen, R. Lan, J. Humphreys, G. Jeerh, S. Tao, Investigation of perovskite oxide SrFe0.8Cu0.1Nb0.1O3-δ as cathode for a room temperature direct ammonia fuel cell, International, J. Hydrog Energy 44 (2019) 26554–26564.

[25] M.H.M.T. Assumpção, S.G. da Silva, R.F.B. De Souza, G.S. Buzzo, E.V. Spinacé, M. C. Santos, A.O. Neto, J.C.M. Silva, Investigation of PdIr /C electrocatalysts as anode on the performance of direct ammonia fuel cell, J. Power Sources. 268 (2014) 129–136.

[26] M.H.M.T. Assumpção, S.G. da Silva, R.F.B. de Souza, G.S. Buzzo, E.V. Spinacé, A. O. Neto, J.C.M. Silva, Direct ammonia fuel cell performance using PtIr/C as anode electrocatalysts, Int. J. Hydrog. Energy 39 (10) (2014) 5148–5152.

[27] O. Siddiqui, I. Dincer, Investigation of a new anion exchange membrane-based direct ammonia fuel cell system, Fuel Cells 18 (4) (2018) 379–388.

[28] C.A. Hepburn, P. Vale, A.S. Brown, N.J. Simms, E.J. McAdam, Development of on-line FTIR spectroscopy for siloxane detection in biogas to enhance carbon contactor management, Talanta 141 (2015) 128–136.

[29] Y. Liu, H.H. Ngo, W. Guo, L. Peng, D. Wang, B. Ni, The roles of free ammonia (FA) in biological wastewater treatment processes: a review, Environ. Int. 123 (2019) 10–19.

[30] J. Pátek, J. Klomfar, Simple functions for fast calculations of selected thermodynamic properties of the ammonia-water system, Int. J. Refrig. 18 (4) (1995) 228–234.

[31] R.L. Stephenson, J.B. Blackburn, The Industrial Wastewater Systems Handbook, CRC Press, 2018.

[32] R.G. Bates, G.D. Pinching, Acidic dissociation constant of ammonium ion at 0 to 50 C, and the base strength of ammonia, J. Res. Natl. Bur. Stand. 42 (5) (1949) 419, https://doi.org/10.6028/jres.042.037.

[33] A.M. Hulme, C.J. Davey, S. Tyrrel, M. Pidou, E.J. McAdam, Transitioning form electrodialysis to reverse electrodialysis stack design for energy generation from high concentration salinity gradients, Energy Convers. Manage. 244 (2021) 114493.

[34] T.H. Christensen, P. Kjeldsen, P.L. Bjerg, D.L. Jensen, J.B. Christensen, A. Baun, H.-J. Albrechtsen, G. Heron, Biogeochemistry of landfill leachate plumes, Appl. Geochem. 16 (7–8) (2001) 659–718.

[35] R. Parsons, T. VanderNoot, The oxidation of small organic molecules A survey of recent fuel cell related research, J. Electroanal. Chem. Interf. Electrochem. 257 (1–2) (1988) 9–45.

[36] E.H. Yu, U. Krewer, K. Scott, Principles and materials aspects of direct alkaline alcohol fuel cells, Energies 3 (8) (2010) 1499–1528.

[37] D.R. Lide, CRC Handbook of Chemistry and Physics, CRC Press, Boca Raton, FL, 2005.

[38] A.D. Santamaria, M. Mortazavi, Aqueous ammonia wetting of gas-diffusion media for electrochemical cells, J. Electrochem. Soc. 167 (2020) 104507.

[39] G. Mulder, P. Coenen, A. Martens, J. Spaepen, Market-ready stationary 6 kW generator with alkaline fuel cells, ECS Trans. 12 (1) (2008) 743–753.

[40] O. Siddiqui, I. Dincer, Development and performance evaluation of a direct ammonia fuel cell stack, Chem. Eng. Sci. 200 (2019) 285–293.

[41] D. Auty, A. Moore, Digestion and greenhouses – synergistic resource recovery, in: 18th European Biosolids & Organic Resources Conference & Exhibition, 2003.

[42] R. Chen, S. Zheng, Z. Lin, Y. Liu, Z. Wang, Performance study of direct ammonia fuel cell based on PtIr/C anode catalyst, Acta Chim. Sin. 79 (2021) 1286–1292.

[43] X. Tian, Z. Gao, H. Feng, Z. Zhang, J. Li, A. Wang, Efficient nutrient recovery/ removal from real source separated urine by coupling vacuum thermal stripping with activated sludge processes, J. Clean. Prod. 220 (2019) 965–973.

[44] J. Foley, P. Lant, Direct methane and nitrous oxide emissions from full-scale wastewater treatment systems, Occasional Paper No. 24, 2009, Water Services Association of Australia.

[45] H.W. Choi, S.I. Na, S. Bin Hong, Y. Chung, D.K. Kim, M.S. Kim, Optimal design of organic Rankine cycle recovering LNG cold energy with finite heat exchanger size, Energy 217 (2021) 119268.

[46] J.F. Richardson, J.H Harker, J.R. Backhurst, J.M. Coulson, Coulson and Richardson's Chemical Engineering Volume 2, Fifth ed., Butterworth-Heinemann, Oxford, 2002.

[47] H. Bannwarth, Liquid Ring Vacuum Pumps and Liquid Ring Compressors – Chapter 3, first ed., Wiley VCH, Weinheim, 2005.